27
3-19-82
EW2HCaptoNTIS

I-2032

UCID-19270 MASTER

TEST AND ANALYTICAL RESULTS OF A NEW BOLT CONFIGURATION FOR A DIAGNOSTIC/DEVICE CANISTER CONNECTION

Lola Boyce
Engineering Mechanics Section

September, 1981

Lawrence Livermore Laboratory

Work performed under the auspices of the U.S. Department of Energy by the Lawrence Livermore Laboratory under Contract W-7405-Eng-48.

CONTENTS

UCID--19270

DE82 008969

TEST AND ANALYTICAL RESULTS OF A NEW BOLT CONFIGURATION FOR A DIAGNOSTIC/DEVICE CANISTER CONNECTION

EXECUTIVE SUMMARY

Underground nuclear explosive tests conducted by Lawrence Livermore National Laboratory at the Nevada Test Site utilize a nuclear device canister suspended from a canister containing diagnostic equipment. The diagnostic canister includes channels that are welded to a thick annular end plate bolted to the device canister.

Previously these diagnostic canisters were designed individually for each test. To reduce costs, a standardized canister design consisting of a family of standard components is being developed. As part of this standard canister design development, both numerical analysis and actual test data were undertaken for a portion of the bolted connection between canisters, to arrive at an optimum design.

The connection, as originally configured, was investigated by Gerhard.[1] It was noted the load in the bolt closest to the channel was higher than the load in the more distant bolt, indicating the possibility of sequential bolt failure. Also, the bolt loads produced a large bending moment in the canister plate. Therefore, it was recommended that the bolts be repositioned such that the large plate bending moment is reduced and the bolts share the load more evenly. This new bolt configuration was tested and numerically analyzed. The results for this bolt configuration are presented and compared with those for the connection as originally configured in the body of the paper.

Actual test data were obtained from a full-scale model of a 45° section of the canister consisting of one channel and four nearby bolts. The test specimen was contructed, instrumented, loaded, and tested by the Engineering Science Division of the Laborstory. It was modified for the new bolt configuration by drilling additional bolt holes in the plate sections. Displacement transducers and strain gages placed at key locations provided data on end plate separations, stresses, and bolt loads.

Analytical results were obtained from a finite element model of the same canister section, utilizing all possible symmetry planes, together with a structural analysis, finite element computer code. This model was modified for the new bolt configuration. Displacements and stresses for all elements

of the model were available. Selected elements corresponding to test specimen locations provided direct comparisons with test results.

Correspondence of results for test and analysis is reasonably good for bolt loads, end plate displacements, and stresses located a distance from the welded channel end plate connection. Poorer correlation exists for results close to the weld. These remarks hold true for both bolt configurations.

The new bolt pattern for the connection has several advantages over the old design, including reduced and more evenly distributed bolt loads, smaller end plate separation, and significant reduction of end plate horizontal stresses. Also, the interplate bearing force and moment are significantly reduced. The plate contact area is increased substantially and its centroid location provides for increased static stability of the connection.

ABSTRACT

Underground nuclear explosive tests utilize a nuclear device canister suspended from a canister containing diagnostic equipment. A standard design for these canisters and their connection is being developed by the Nuclear Test Engineering Divisions, Test Systems Section of Lawrence Livermore National Laboratory. Test and analysis of a new bolt configuration for a portion of this bolted canister connection have been carried out and results are presented and compared for channel loads of 100 000 and 200 000 lb. When results for this connection design are compared with an earlier one, significant reductions are found in bolt loads, end plate separations, and certain stresses and moments.

INTRODUCTION

Underground nuclear explosive tests conducted by Lawrence Livermore National Laboratory at the Nevada Test Site utilize a nuclear device canister suspended from a canister containing diagnostic equipment. The diagnostic canister, as depicted in Fig. 1, includes channels that are welded to a thick annular end plate bolted to the device canister.

Previously these diagnostic canisters were designed individually for each test. To reduce costs, a standardized canister design consisting of a family of standard components is being developed. As part of this standard canister design development, both numerical analysis and actual test data were undertaken for a portion of the bolted connection between canisters (Fig. 2) to arrive at an optimum design.

The connection, as configured in Fig. 2, was investigated by Gerhard.[1] It was noted the load in the bolt closest to the channel was higher than the load in the more distant bolt indicating the possibility of sequential bolt failure. Also, the bolt loads produced a large bending moment in the canister plate. Therefore, it was recommended that the bolts be repositioned such that the large plate bending moment is reduced and the bolts share the load more evenly. This new bolt configuration, Fig. 3, was tested and numerically analyzed. The results for this bolt configuration are presented and compared with those for the connection as originally configured.

TEST SPECIMEN AND ANALYTICAL MODEL

Actual test data were obtained from a full-scale model of a 45° section of the canister consisting of one channel and four nearby bolts. The test specimen was constructed, instrumented, loaded, and tested by the Engineering Science Division of the Laboratory. It was modified for the new bolt configuration by drilling additional bolt holes in the plate sections. A schematic of the test specimen is given in Fig. 4. Further geometric details are given in Ref. 1. Displacement transducers and strain gages placed at key locations (see Figs. 5 through 9) provided data on end plate separations, stresses, and bolt loads.

Analytical results were obtained from a finite element model of the same canister section, utilizing all possible symmetry planes, together with a

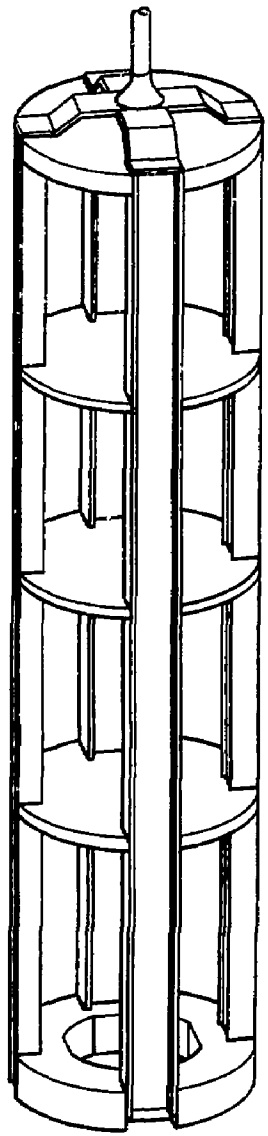

FIG 1. General configuration of a diagnostic canister. The interior bulkheads are used for stiffening and mounting diagnostic instruments; the device canister is suspended from the bottom of the canister.

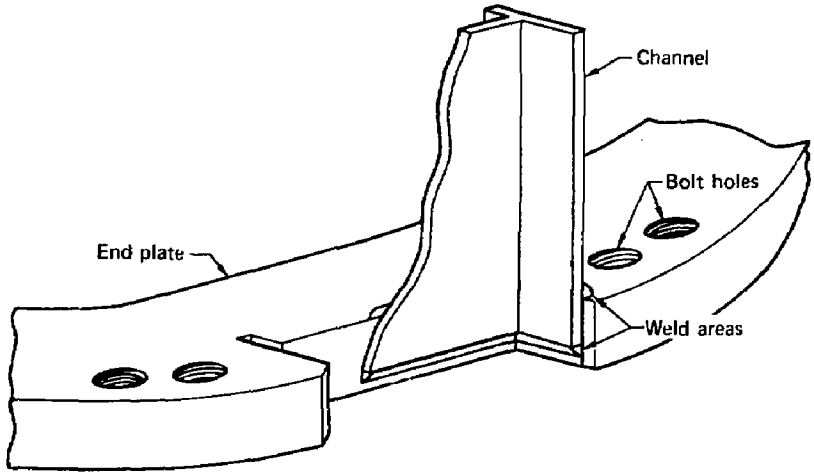

FIG. 2. Channel/end plate joint for the old bolt configuration (Ref. 1).

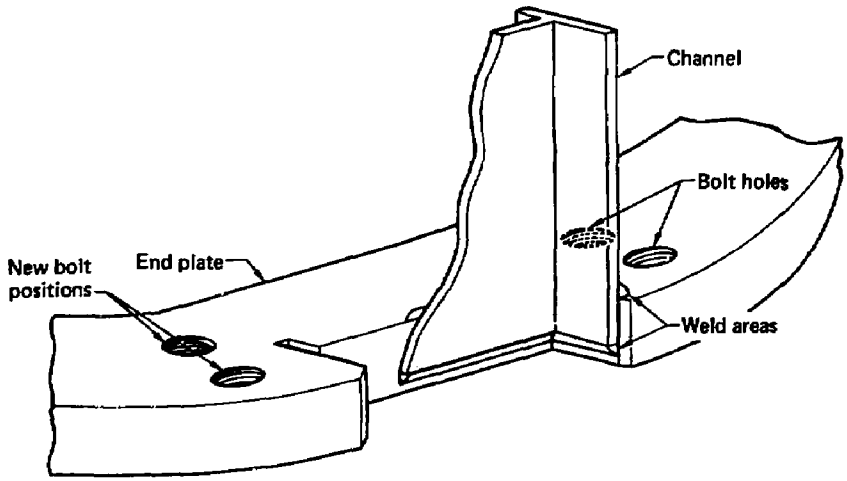

FIG. 3. Channel/end plate joint for the new bolt configuration.

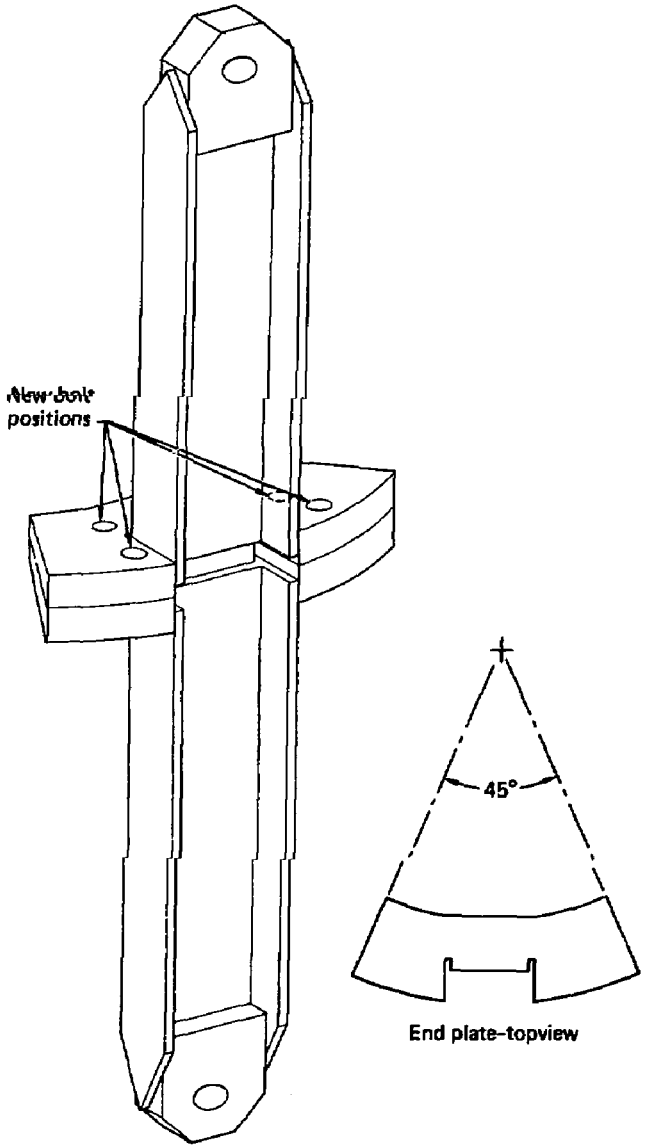

FIG. 4. Test specimen for pull test. A "point" load is applied through the eye holes. The end plates are truncated to a 45° symmetrical section.

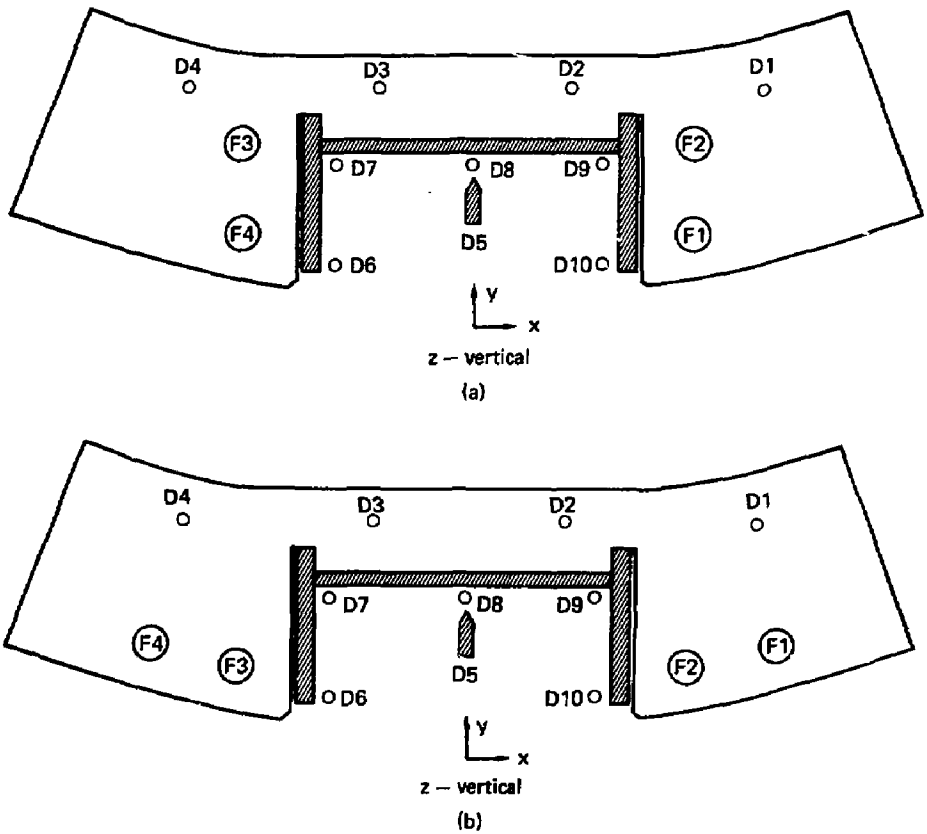

FIG. 5. Load bolt locations (F1 to F4) and displacement transducer locations (D1 to D10) for (a) the new bolt configuration and (b) the old bolt configuration.

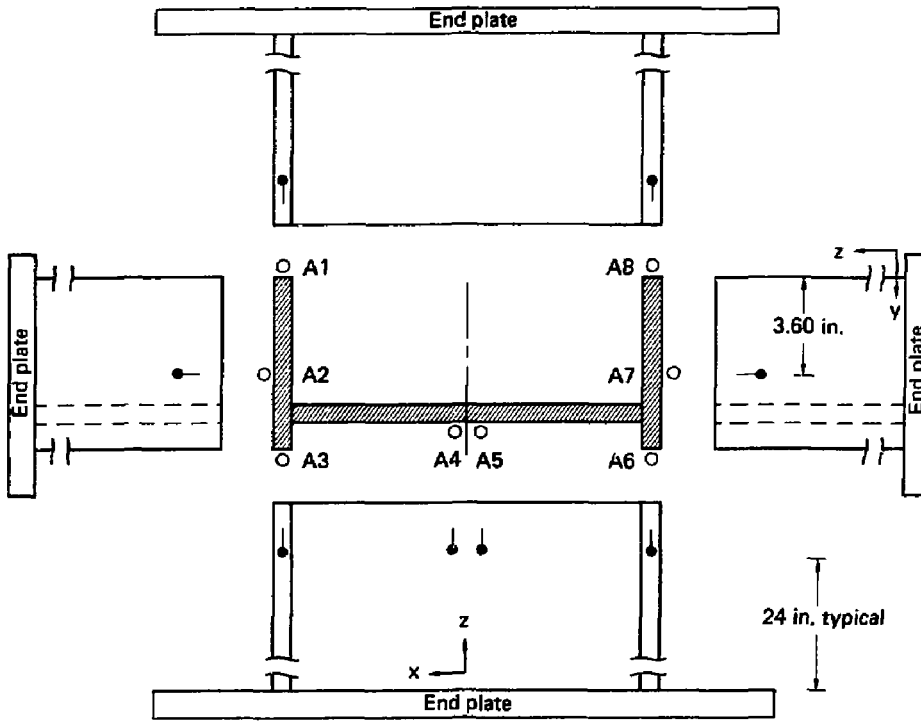

FIG. 6. Uniaxial strain gage location (A1 to A8) in the z direction 24 in. above the end plate.

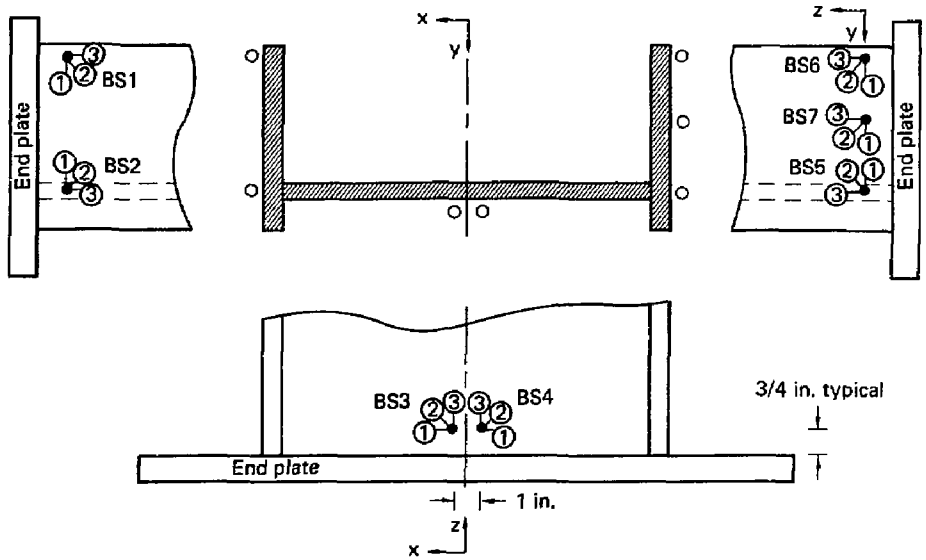

FIG. 7. Rosette strain gage locations (BS1 to BS6) 3/4 in. above the end plate outside the channel.

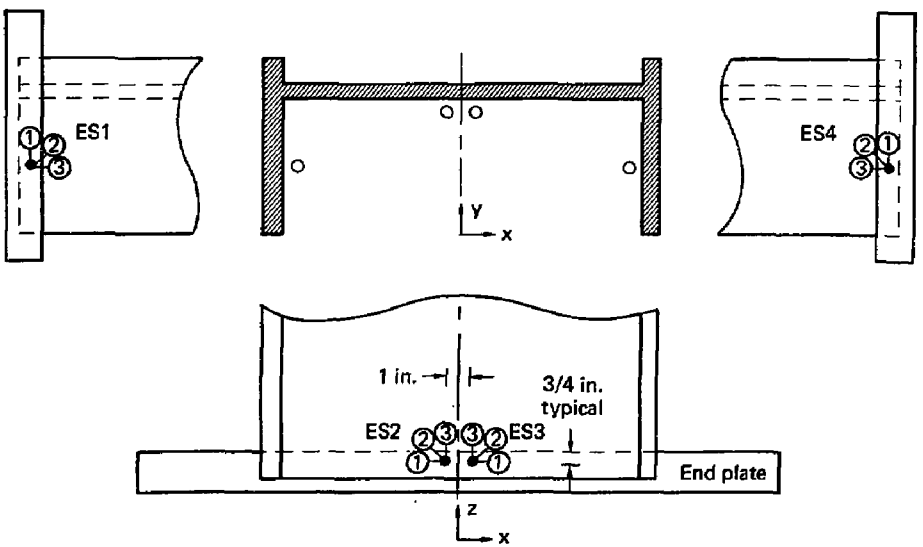

FIG. 8. Rosette strain gage locations (ES1 to ES4) 3/4 in. above the end plate inside the channel.

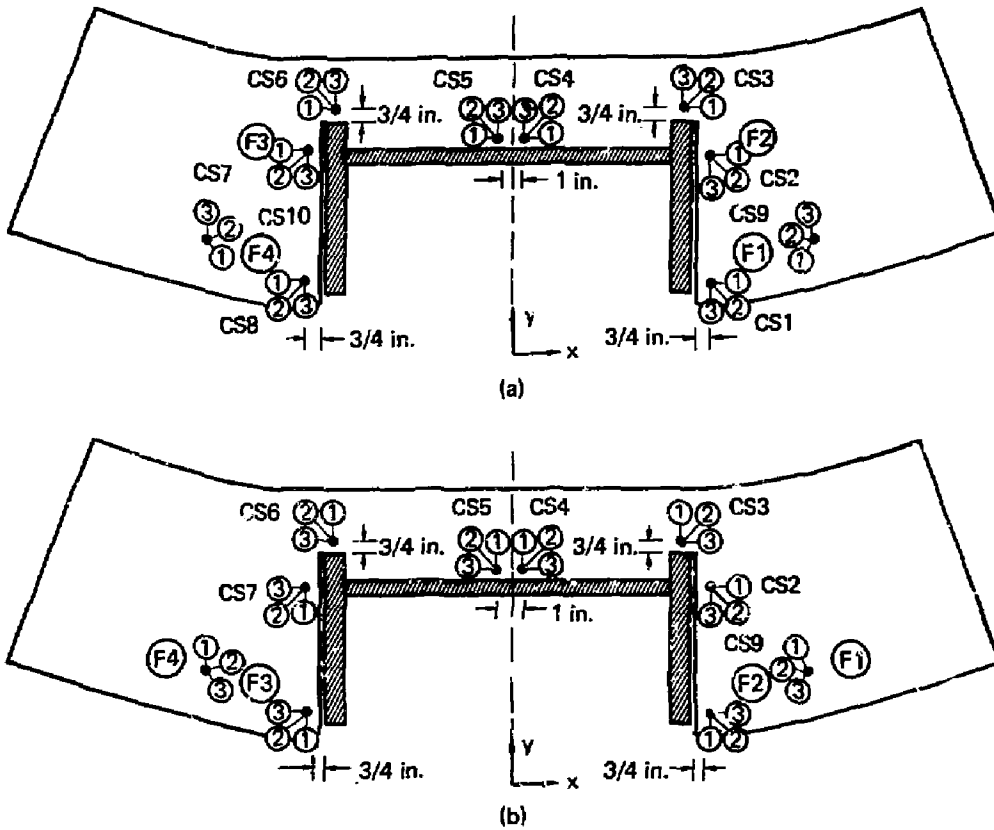

FIG. 9. Rosette strain gage locations (CS1 to CS10) on end plate top surface for (a) the new bolt configuration and (b) the old bolt configuration.

structural analysis, finite element computer code. This model was modified for the new bolt configuration and is shown in Fig. 10. Reference 1 also includes a detailed discussion of the finite element model. Displacements and stresses for all elements of the model were available. Selected elements corresponding to test specimen locations provided direct comparisons with test results.

CONNECTION GEOMETRY AND STATICS

The geometry of the channel/end plate joint is given in Fig. A-1 of Appendix A. The channel centroid location C_B is the point through which both the test specimen and the analytical model are loaded.

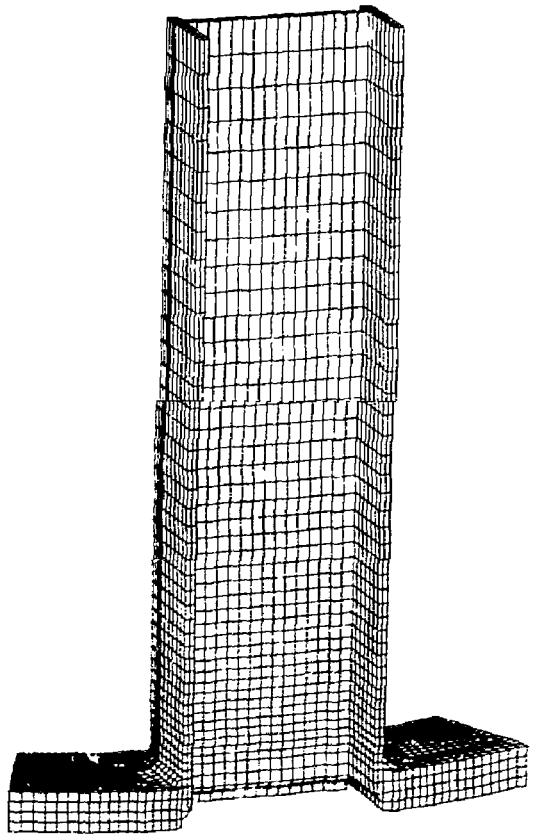

FIG. 10. Analytical finite element model of 45° canister section.

The statics of the connection mechanism include an interplate bearing force $\overline{A}$ found by vertical equilibration of this bearing force together with the bolt loads and the channel load. Furthermore, the bolt loads create a moment in the x direction $\overline{M}_B$ that is balanced by an equivalent moment $\overline{M}_A$ found by location of the interplate bearing force at an appropriate distance from the channel centroid. These static mechanisms are illustrated schematically for both the old and the new bolt configurations in Fig. 11.

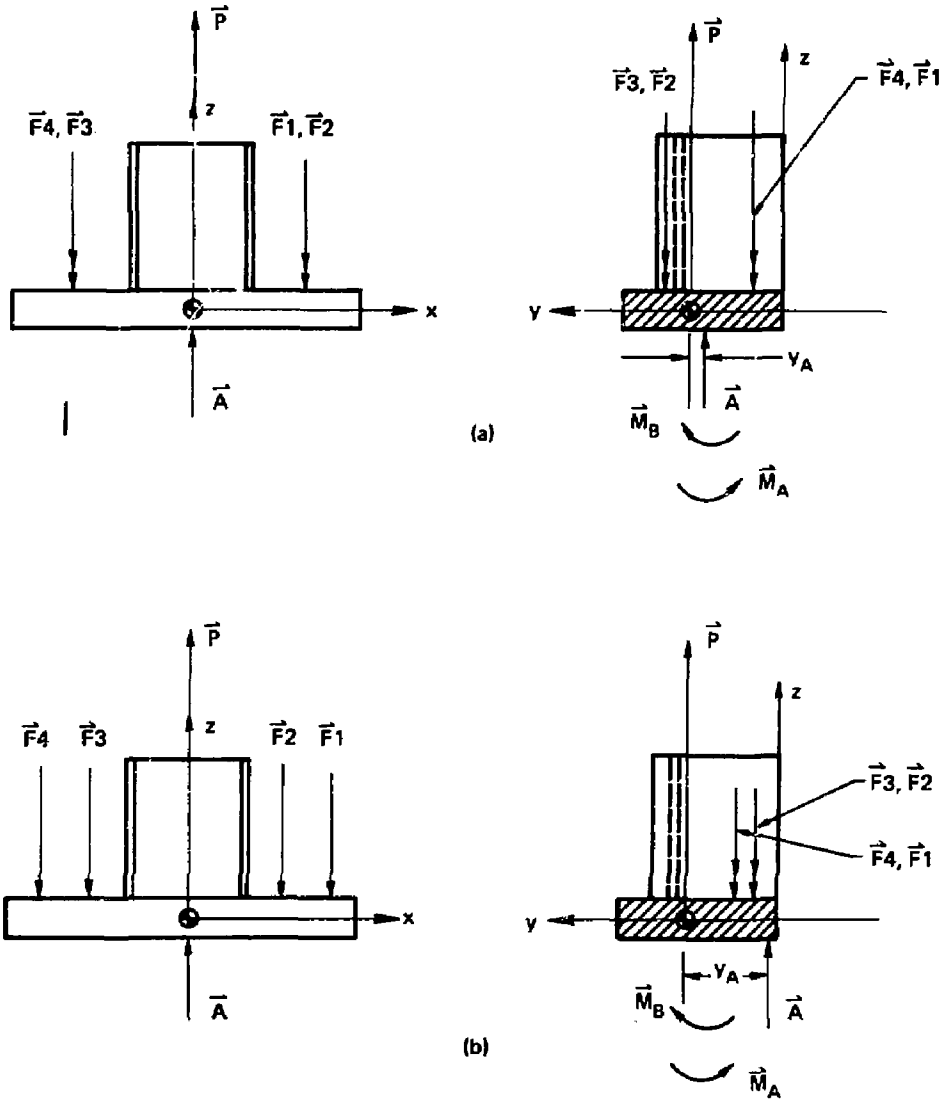

FIG. 11. Static joint mechanism showing bolt loads, $\vec{F}1$ to $\vec{F}4$, externally applied channel load, $\vec{P}$, interplate bearing force, $\vec{A}$, the moment due to bolt loads, $\vec{M}_B$, and the moment due to the interplate bearing force, $\vec{M}_A$.

TEST RESULTS

Full-scale model testing was performed under the supervision of T. Miller of the Engineering Measurements Section of the Mechanical Engineering Department's Engineering Sciences Division. A total of 13 tests were made utilizing various bolt configurations and maximum channel loadings. For example, the new bolt configuration (Fig. 3) for a maximum load of about 200 000 lb was tested on September 11, 1980; computer printouts of the results are labeled "Test No. 12." The old bolt configuration (Fig. 2) for a maximum load of about 110 000 lb was tested on July 15, 1980; printouts are labeled "Canister-1." Tests for other bolt configurations and maximum loads were also executed; however, their results are not discussed in this report.

Initially, the bolts were preloaded and then a "point" load was slowly applied and removed from the eye holes of the test specimen. For the old bolt configuration (Canister-1) the average bolt preloads were about 68 000 lb for all bolt locations and the channel was loaded to a maximum of about 110 000 lb. Data for a 100 000-lb load are presented in Ref. 1. For the new bolt configuration (Test No. 12) the average bolt preloads were 69 800 lb for location F1/F4 (Fig. 5) and 69 400 lb for locations F2/F3 (Fig. 5). The channel was loaded to a maximum of about 200 000 lb. Data for both 100 000- and 200 000-lb channel loads are presented. Table 1 gives the bolt loads and end plate separations for a channel load of 100 000 lb for locations depicted in Fig. 5(a). Table 2 gives the axial stresses at a distance of 24 in. above the end plate for the same loading. The locations of these stresses are given in Fig. 6. Table 3 gives the axial stresses, principal stresses, and maximum shear stresses also for 100 000 lb. These stress locations are given in Figs. 7, 8, and 9(a). Analogous results for a channel load of 200 000 lb are given in Tables 4, 5, and 6. Test results for the old bolt configuration (Canister-1) are given in Ref. 1.

Observation of the test results indicate the presence of a moment in the vertical (z) direction in the channel web and one flange near the end plate. This moment can be implied by comparison of stresses located on opposite sides of the channel web and flange as illustrated in Fig. 12 for a channel load of 100 000 lb. A schematic of the deformed channel is shown by dashed lines and greatly exaggerated. Similar results hold for the test results at a 200 000 lb channel load. The significance of this channel moment is that it tends to deform both the channel and end plate such that the end plate loses some of

TABLE 1. Bolt loads and end plate separations for a channel load of 100 000 lb for locations depicted in Fig. 5(a).

Gage	Measurement
Average bolt loads (lb)	
F1	71 460
F2	71 026
F3	70 700
F4	72 047
Displacement transducers (mil)[a]	
D1	-0.1044
D2	4.447
D3	3.040
D4	-0.0840
D5	-10.38
D6	5.137
D7	5.890
D8	8.534
D9	5.453
D10	5.137

[a] 1 mil = 0.001 in.

its curvature. In this manner the test specimen does not accurately model the real canister geometry because no constraint is imposed along the plate edges that, for the real canister, would be rigidly attached to adjoining channel/end plate sections.

Examination of the test results for channel stresses located 24 in. above the end plate resulted in two significant observations. First, the stress present at the neutral axis (locations A2/A7, Fig. 6) of the channel is entirely due to an axial force. This actual axial force was found to be significantly lower than the externally applied load indicated by the load cell. For the old bolt configuration the actual axial force was 90 900 lb (100 000-lb channel load) and for the new bolt configuration it was 86 600 lb

TABLE 2. Axial strains and stresses 24 in. above the end plate for a channel load of 100 000 lb[a] for locations given in Fig. 6.

Gage	Strain (10^{-6} in./in.)	σ_z(psi)
A1	220.4	6392
A2	226.8	6577
A3	243.4	7059
A4	233.6	6774
A5	235.4	6827
A6	252.2	7314
A7	234.8	6809
A8	220.0	6380

[a] Based on E = 29.0 x 10^6 psi.

for the 100 000-lb load and 172 950 lb for the 200 000-lb load. Hence, although the load cell indicated 100 000 and 200 000 lb, respectively, the axial force present (indicated by strain gages and calculated stresses) was much lower. Conversations with T. Miller confirmed that the load cell had not been calibrated in a very long time and that this fact could definitely have contributed to the low axial loads. Second, the stress gradient in the y direction along the flanges (locations A3/A6, A2/A7, and A1/A8, Fig. 6) indicate the presence of a channel bending-moment in the x direction. Although this stress distribution is not linear, an approximate maximum bending moment may be calculated assuming linearity. For the 100 000-lb channel load this moment is 1224 ft-lb and for the 200 000-lb load it is 3215 ft-lb. It is interesting to note that for the old bolt configuration considered in Ref. 1, this moment is in the minus x direction and is approximately calculated as 2834 ft-lb. Therefore, for the 100 000-lb load, this moment is significantly reduced to 1224 ft-lb for the new bolt configuration.

Inspection of the data for Test No. 12 shows that data channels 128, 134, and 147 gave results that were totally in error. These bad data channels lead to errors for certain stresses presented in Tables 3 and 6. These stresses are cited by superscript a in the tables. Note that only channel 134 (ϵ_3 of CS1) affects axial stresses that are later used for direct comparisons with analytical results. Fortunately, redundancy was provided in the test specimen

TABLE 3. *Axial stresses, principal stresses, and maximum shear stresses for a channel load of* 100 000 lb for locations in Figs. 7, 8, and 9(a).

Gage	μ strain (10^{-6} in./in.)			Axial stresses (psi)			Principal stresses (psi)		Location (deg)	Max shear stress (psi)
	ε_1	ε_2	ε_3	σ_x	σ_y	σ_z	σ_{max}	σ_{min}	θ	τ_{max}
BS1	- 48.2	323.9	457.9	0	2890	14 380	14 980	2 290	-12.6	6 350
BS2	-113.3	205.7	511.5	0	1300	15 480	15 480	1 300	- 0.605	7 090
BS3	28.1	61.9	103.4	1917	0	3 625	3 630	1 912	2.92	859
BS4	22.6	49.2	108.5	1788	0	3 740	3 800	1 720	1.04	1 043
BS5	-122.4	187.0	518	0	1070	15 600	15 600	1 066	0.966	7 270
BS6	-44.6	1816[a]	432	0	2760	13 570	45 370[a]	-29 000[a]	-40.8[a]	37 700[a]
BS7	6.84	382	493	0	5020	16 050	16 810	4 250	-14.3	6 280
CS1	-213	- 66.7	-240[a]	-9240[a]	-9850[a]	0	-5 910[a]	-13 180[a]	42.6[a]	3 640[a]
CS2	-213	- 66.5	10.5	-6800	-1731	0	-1 611	- 6 920	- 8.64	2 660
CS3	- 36.2	- 88.8	23.0	- 950	394	0	1 704	- 2 260	35.1	1 983
CS4	52.3	- 0.422	- 35.1	1354	- 629	0	1 375	- 650	- 5.83	1 013
CS5	46.3	96.7[a]	- 15.2	1353	- 42.5	0	2 620[a]	- 1 314[a]	3.46[a]	1 969[a]
CS6	- 54.1	-140.6	- 4.19	-1795	- 662	0	1 364	- 3 820	38.7	2 590
CS7	-208.6	- 70.1	- 12.4	-6880	-2430	0	-2 250	- 7 060	-11.2	2 410
CS8	-214	- 50.6	25.3	-6690	-1261	0	-1 085	- 6 870	-10.0	2 890
CS9	- 65.6	- 78.7	6.67	--	--	0	144.1	- 2 630	26.9	1 386
CS10	- 57.5	- 46.7	1.88	--	--	0	- 373	- 1 971	16.2	799
ES1	- 60.9	31.3	191.1	0	- 115.7	5 600	5 700	- 217	7.51	2 960
ES2	-107.2	- 31.5	25.4	-3230	0	- 219	- 204	- 3 243	- 4.03	1 520
ES3	-106.7	- 51.7	25.9	-3210	0	- 198.1	- 176.4	- 3 230	4.84	1 526
ES4	- 36.7	70.7	225	0	990	6 940	6 980	951	5.08	3 020

[a] Bad test data.

TABLE 4. Bolt loads and end plate separation for a channel load of 200 000 lb for locations depicted in Fig. 5(*a*).

Gage	Measurements
Average bolt loads (lb)	
F1	80 919
F2	80 447
F3	80 439
F4	82 225
Displacement transducers (mil)[a]	
D1	-0.1195
D2	15.87
D3	15.52
D4	0.1149
D5	-16.91
D6	17.98
D7	17.88
D8	24.18
D9	17.39
D10	17.19

[a] 1 mil = 0.001 in.

TABLE 5. Axial strains and stresses 24 in. above the end plate for a channel load of 200 000 lb[a] for locations given in Fig. 6.

Gage	μ Strain (10^{-6} in./in.)	σ_z(psi)
A1	422.5	12 253
A2	453.1	13 140
A3	498.4	14 454
A4	473.0	13 717
A5	475.6	13 792
A6	513.0	14 877
A7	468.8	13 595
A8	428.5	12 427

[a] Based on E = 29.0 x 10^6 psi.

TABLE 6. Axial stresses, principal stresses, and maximum shear stresses for a channel load of 200 000 lb for locations in Figs. 7, 8, and 9(a).

	μ strain (10^{-6} in./in.)			Axial stresses (psi)			Principal stresses (psi)		Location (deg)	Max shear stress (psi)
Gage	ε_1	ε_2	ε_3	σ_x	σ_y	σ_z	σ_{max}	σ_{min}	θ	τ_{max}
BS1	- 87.0	762.6	1006.3	0	6 970	31 800	33 550	5 190	-14.5	14 180
BS2	-307.5	424.7	1162.4	0	1 340	34 700	34 700	1 340	- 0.107	16 700
BS3	78.6	87.6	135.8	3 870	0	5 170	5 300	3 730	17.2	787
BS4	68.2	70.4	143.7	3 610	0	5 320	5 640	3 290	21.6	1 177
BS5	-320	413	1184.8	0	1 150	35 300	35 300	1 140	0.738	17 100
BS6	-79.2	1272.8[a]	967.3	0	6 840	30 600	41 000[a]	- 3 530[a]	-28.9[a]	22 200[a]
BS7	70.5	900.3	1089.5	0	12 900	36 000	38 100	10 800	-16.1	13 700
CS1	-372	- 63.7	-2905[a]	-40 300[a]	-97 800[a]	0	-23 200[a]	-115 000[a]	25.6[a]	45 900[a]
CS2	-293	3.65	39.4	- 9 120	- 1 570	0	- 549	- 10 140	-19.1	4 790
CS3	25.0	- 97.8	28.4	1 087	1 164	0	3 950	- 1 700	44.6	2 830
CS4	127.3	41.5	- 52.1	3 620	- 451	0	3 620	- 453	1.24	2 040
CS5	120.2	118.8[a]	- 27.6	3 630	274	0	4 300[a]	- 398[a]	22.2[a]	2 350[a]
CS6	9.92	-179.5	- 26.3	65.8	- 756	0	3 560	- 4 550	-42.0	3 910
CS7	-286	- 20.9	- 2.01	- 9 290	- 2 850	0	-1 800	- 10 330	-20.5	4 260
CS8	-184	- 40.3	61.8	-11 850	- 1 731	0	-1 036	- 12 540	-14.2	5 750
CS9	-245.1	-344.8	- [illegible].7	--	--	0	- 269	- 11 060	31.1	5 400
CS10	-232	-282	- [illegible].5	--	--	0	-1 159	- 9 610	28.0	4 220
ES1	-112.3	- 11.72	302	0	- 703	8 700	9 280	- 1 289	13.6	5 290
ES2	-242	- 92.7	[illegible].9	-7 740	0	-2 000	-1 954	- 7 890	- 5.12	2 920
ES3	-246	-121.8	12.78	-7 850	0	-1 978	-1 976	- 7 850	1.15	2 940
ES4	- 57.4	47.7	373	0	1 767	11 530	12 140	1 165	13.5	5 890

[a] Bad test data.

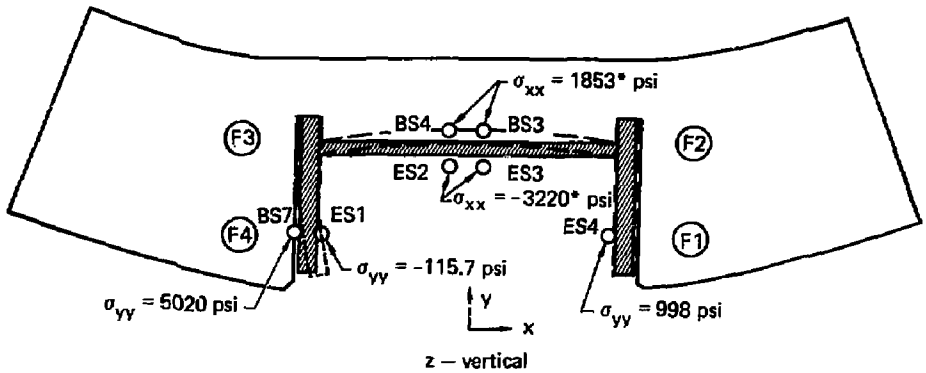

FIG. 12. Test results indicate a vertical channel moment in web and one flange near the end plate. The moment can be implied by comparisons of stresses located on opposite sides of the channel. A schematic of the deformed channel is shown by dashed lines and is greatly exaggerated. The data illustrated are for a 100 000-lb channel load. Asterisk (*) is for average value.

(through geometric symmetry) and channel 155 (ε_3 of CS8), for instance, could be substituted for channel 134. Tables 3 and 6 show that all bad channels lead generally to very large values of principal stresses and maximum shear stresses. Comparison of Test No. 12 with Test No. 13 (simply a rerun of 12) showed the repeatability of data for good channels but a complete lack of correspondence for bad data channels.

Finally, other factors that may affect the quality of data obtained from test specimen were gleaned from conversations with T. Miller. Test displacements turned out to be in the highly nonlinear range of the displacement transducers. Bolt holes F2/F3 [Fig. 5(a)] were drilled (in house) after manufacturing and testing of the old bolt configuration was complete and may not be as precisely sized and located as the old bolt locations, F1/F4 and F2/F3 [Fig. 5(b)]. Also, the tests were manually operated and hence subject to operator variability.

ANALYTICAL RESULTS

Analytical results were obtained by applying the SAP4[2] structural analysis, linear finite element code to the finite element model in Fig. 10.

Rationale for the choice of the SAP4 code is given in Ref. 1. Results are presented for both 100 000- and 200 000-lb channel loads.

The SAP4 code requires an iterative solution process wherein successive guesses for the interplate contact area are made until the correct area is obtained. The contact area is defined by stiff boundary spring elements located at nodes within the area. By observing all possible contact surface nodal displacements, the next guess for contact area is made. In this manner the final contact area and hence the final analytical solution is obtained. Figures 13 and 14 depict the contact area for 100 000- and 200 000-lb channel loads, respectively.

The analytical solution includes bolt loads, given by the summation of forces in eight three-dimensional truss members simulating each bolt, end plate separations, given by displacement of interplate nodes, and stresses, given by stresses located at the centroid of three-dimensional solid elements.

The old and new bolt configurations are modeled by finite element models generated by the automatic mesh generator SLIC.[3] The final iterated analyses for both bolt configurations and for the channel loads considered, are contained in computer input and output files listed in Table A-1 in Appendix A. Bolt preloads for both bolt configurations were determined from an end plate/bolt model (generated by SLIC) and calculated by SAP4. These files are also listed in Table A-1.

Graphical observation of analytical results is possible through computer-drawn illustrations of the deformed connection. Figures 15 and 16 illustrate end plate bending and separation from two perspectives for a 100 000-lb channel load. Comparison of these figures with Fig. 4 of Ref. 1 (repeated here for convenience as Fig. 17) indicates that bending is much reduced, thereby greatly increasing contact area, and the maximum end plate separation is reduced significantly from 0.038 to 0.007 in.

Examination of the analytical results does not indicate a vertical moment (z direction) near the end plate in the channel web and only small moments in the flanges confined to the ends of the flange farthest from the web. Hence the channel generally maintains its undeformed shape except that the ends of the flanges rotate inward somewhat. This is illustrated in Fig. 18 for a channel load of 100 000 lb. Very similar results are found for a 200 000-lb channel load.

Analytical results for channel stresses located 24 in. above the end plate indicate that the axial force present is essentially identical to the

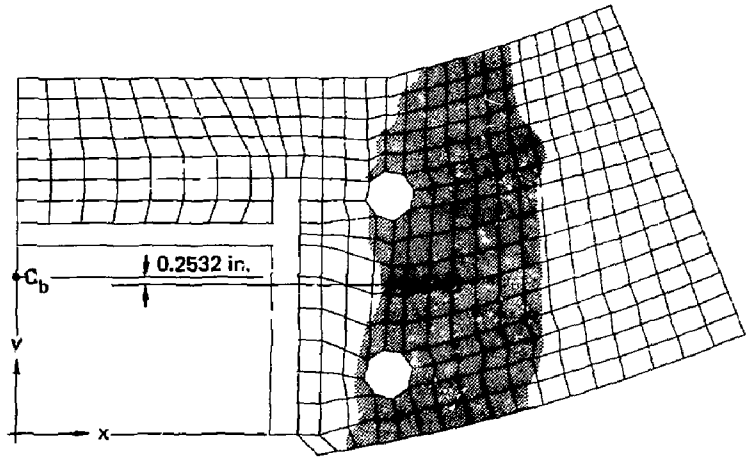

FIG. 13. Final analytical results indicate the shaded interplate contact area for a channel load of 100 000 lb for the new bolt configuration.

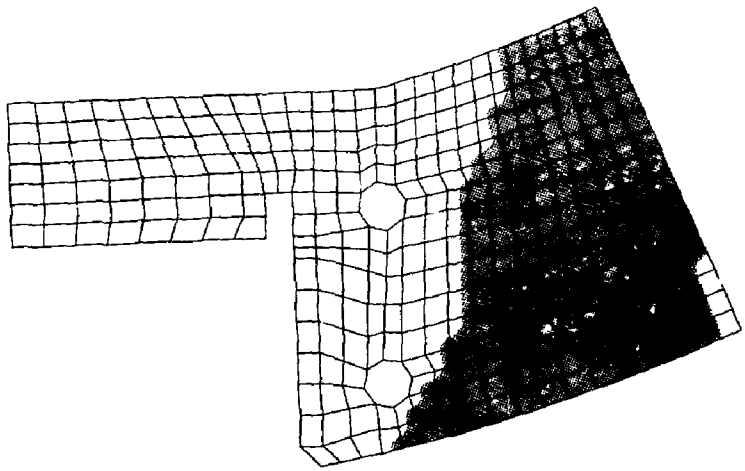

FIG. 14. Final analytical results indicate the shaded interplate contact area for a channel load of 200 000 lb for the new bolt configuration.

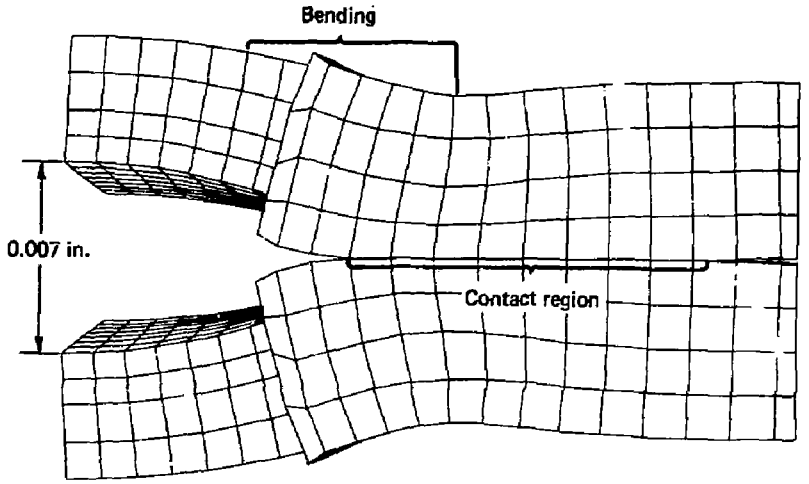

FIG. 15. End plate bending and separation for 100 000-lb channel load for new bolt configuration. The maximum separation was 0.007 in.

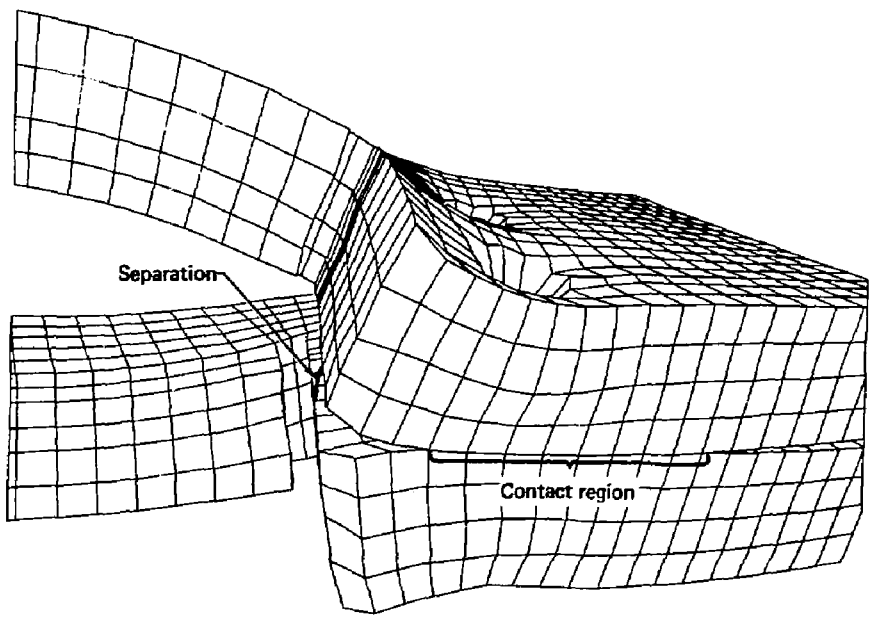

FIG. 16. End plate bending and separation for a 100 000-lb channel load, oblique perspective, for the new bolt configuration The end plate separated over approximately 75% of the original contact area.

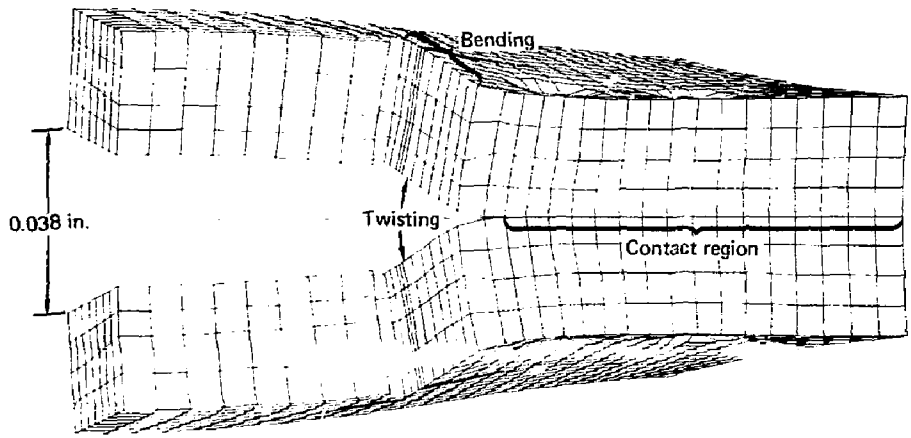

FIG. 17. (Fig. 4, Ref. 1, old bolt configuration) End plate bending and separation. Localized bending occurred near the bolts, and the end plate separated over approximately 90 percent of the original contact area. The maximum separation was 0.038 in. for a channel load of 100 kips.

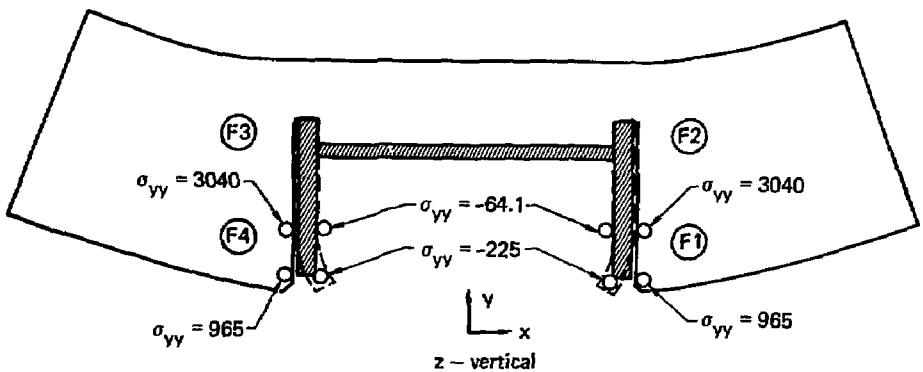

FIG. 18. Analytical results indicate that the channel maintains its undeformed shape near the end plate except for the ends of the flanges. A vertical moment can be implied by comparisons of stresses located on opposite sides of the channel. A schematic of the deformed channel is shown by shaded area and is greatly exaggerated. The data illustrated are for a 100 000-lb channel load.

externally applied channel force input to the analysis code. Also the channel bending moments in the x direction are very small or absent. These two results hold for all channel loads and bolt configurations considered here and in Ref. 1.

COMPARISONS OF TEST RESULTS AND ANALYTICAL SOLUTIONS FOR THE NEW BOLT CONFIGURATION

Test specimen data give results at selected transducer and strain gage locations. Analytical solutions yield results at many more nodal and element locations. In order to make a direct comparison of test and analytical results, it is necessary, for example, to select the node closest to transducer locations for end plate separation comparisons, and to select the element whose boundaries include the strain gage location for stress comparisons. Hence comparisons are somewhat approximate. Furthermore, it should be noted that while strain gages give stresses located on the surface of the test piece, analysis results in stress values at the centroid of the element, a point contained within the volume of the analytical model.

Test specimen data give redundant results due to the symmetry of the test piece. For example strain gage locations BS1 and BS6 (Fig. 7) provide information about the same geometric point on the channel flange. Hence, for comparison purposes symmetrical test data values have been averaged.

Direct comparisons of test and analytical results for the new bolt configurations for a 100 000-lb channel load are given in Figs. 19 through 25. Analogous comparisons for 200 000 lb are given in Figs. 26 through 32. Figures 19 and 26 show that bolt loads and end plate displacements agree reasonably well except for the opposing lateral motions of the end plate given at location D5. Figures 20 and 27 again indicate reasonable correspondence for stresses 24 in. above the end plate. However, as noted previously, test results indicate a bending moment in the channel which is essentially absent for the analysis. Figures 21 and 28 give a much poorer correlation of test and analysis; however, trends for tension and compression are generally maintained. Figures 22, 24, 29, and 31 give stresses in the vertical (z) direction near the end plate that roughly correspond. A bending moment is indicated by the tension-compression change through the web thickness and, markedly, by an analytically indicated stress gradient along the length of the

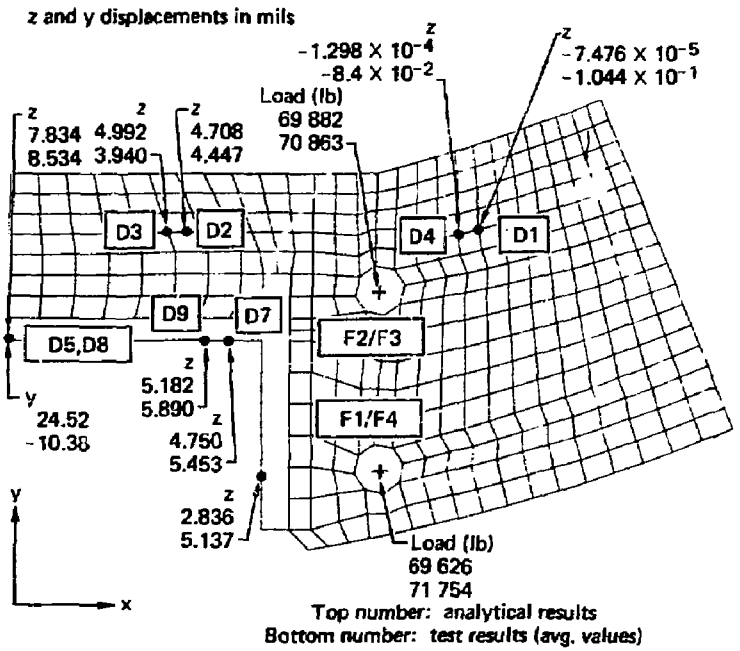

FIG. 19. Bolt loads and end plate displacements for a channel load of 100 000 lb for the new bolt configuration.

flange. It is interesting to note that the highest stress present is analytically predicted for the short end of the flange. Unfortunately there is no test data available at this location. Figures 23, 25, 30, and 32 illustrate stresses in the horizontal (x and y) direction near the end plate. Correspondence of test and analysis is again rather poor; however, both data reach maximum values about midway along the flange with lesser stresses at the ends. Bending moments associated with these stresses have been previously discussed and can be compared for test and analytical results with Figs. 12 and 18.

In summary, bolt loads, end plate displacements, and vertical stresses (σ_{zz}) 24 in. above the plate yield test and analytical values that correspond well. Stress comparisons for locations near the welded joint of the channel/end plate show a much poorer correlation; however, vertical

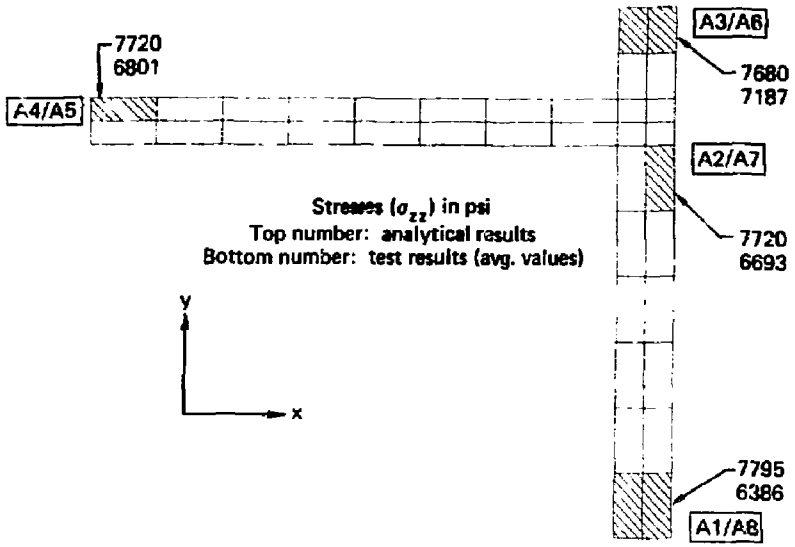

FIG. 20. Vertical channel stresses (σ_{zz}) located 24 in. above the end plate for a channel load of 100 000 lb for the new bolt configuration.

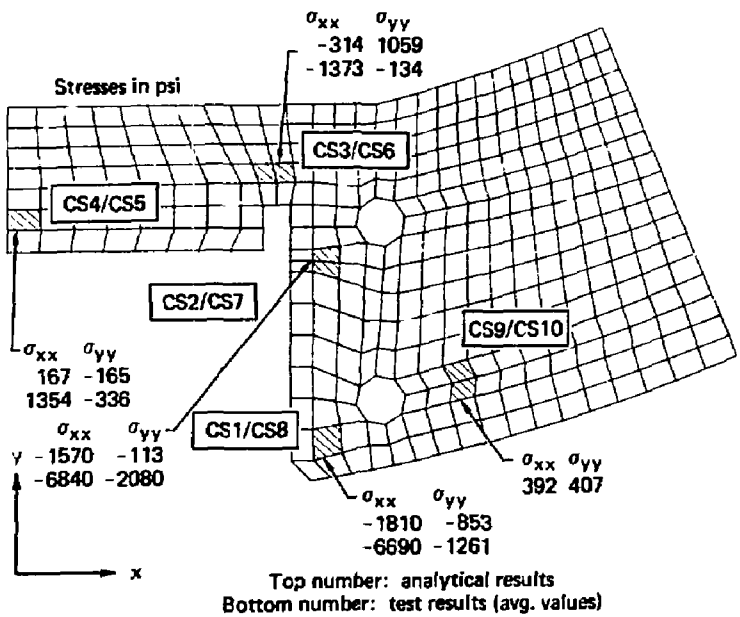

FIG. 21. Horizontal stresses (σ_{xx} and σ_{yy}) for end plate top surface for a channel load of 100 000 lb for the new bolt configuration.

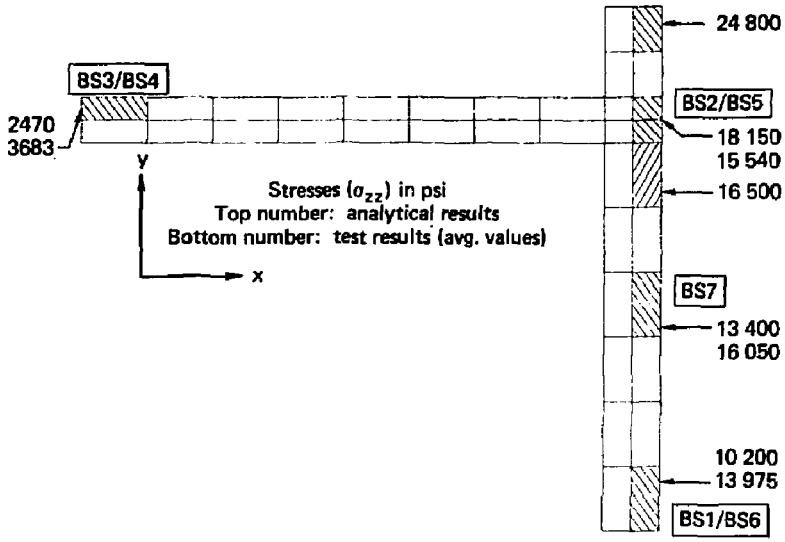

FIG. 22. Vertical stresses (σ_{zz}) for the outside of the channel located 3/4 in. above the end plate for a channel load of 100 000 lb for the new bolt configuration.

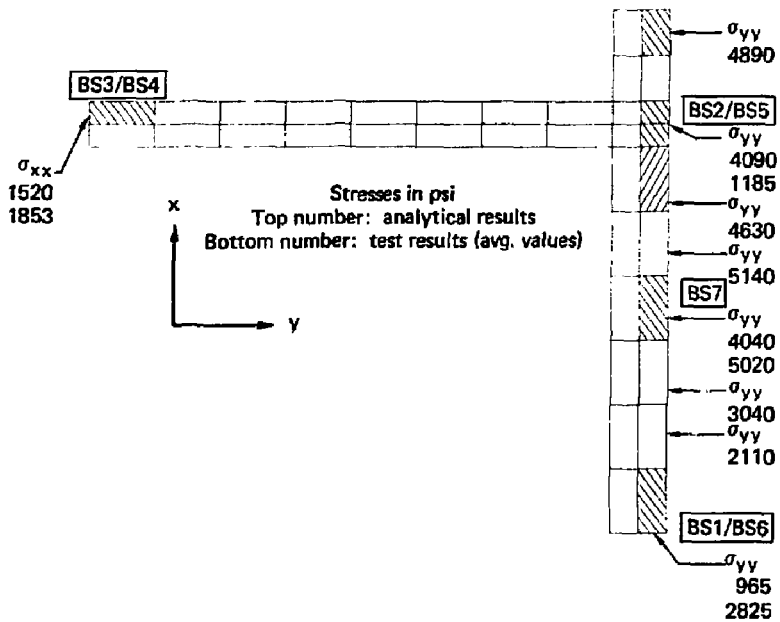

FIG. 23. Horizontal stresses (σ_{xx} and σ_{yy}) for the outside of the channel located 3/4 in. above the end plate for a channel load of 100 000 lb for the new bolt configuration.

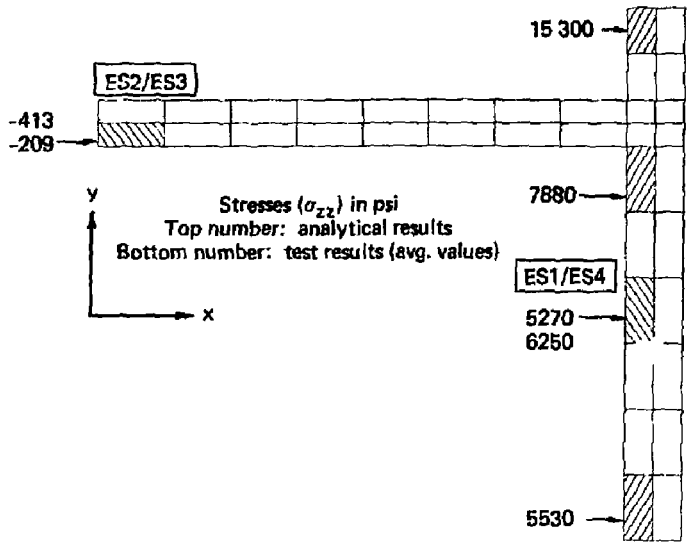

FIG. 24. Vertical stresses (σ_{zz}) for the inside of the channel located 3/4 in. above the end plate for a channel load of 100 000 lb for the new bolt configuration.

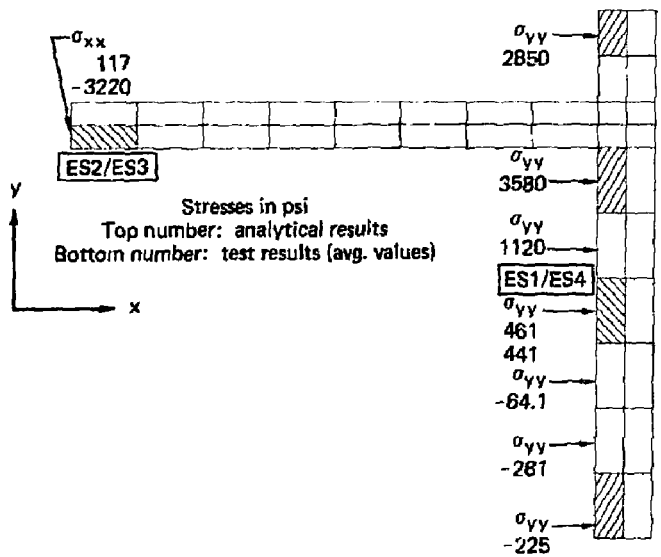

FIG. 25. Horizontal stresses (σ_{xx} and σ_{yy}) for the inside of the channel located 3/4 in. above the end plate for a channel load of 100 000 lb for the new bolt configuration.

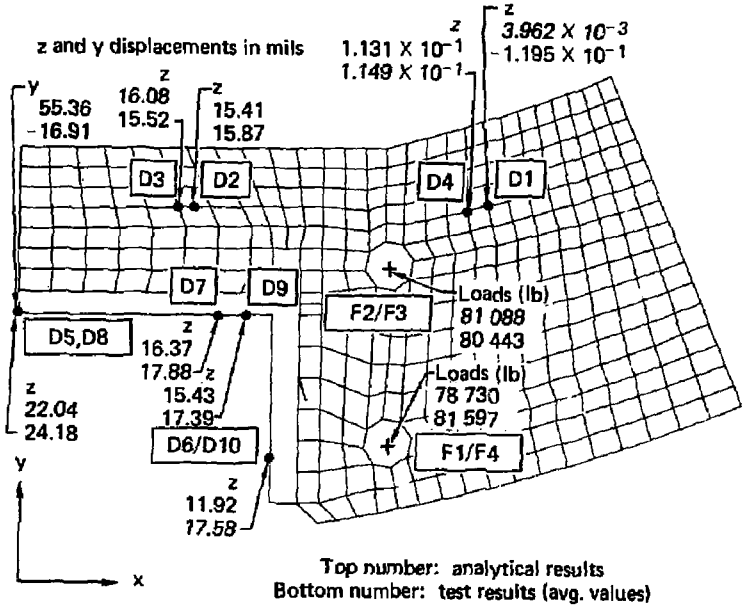

FIG. 26. Bolt loads and end plate displacements for a channel load of 200 000 lb for the new bolt configuration.

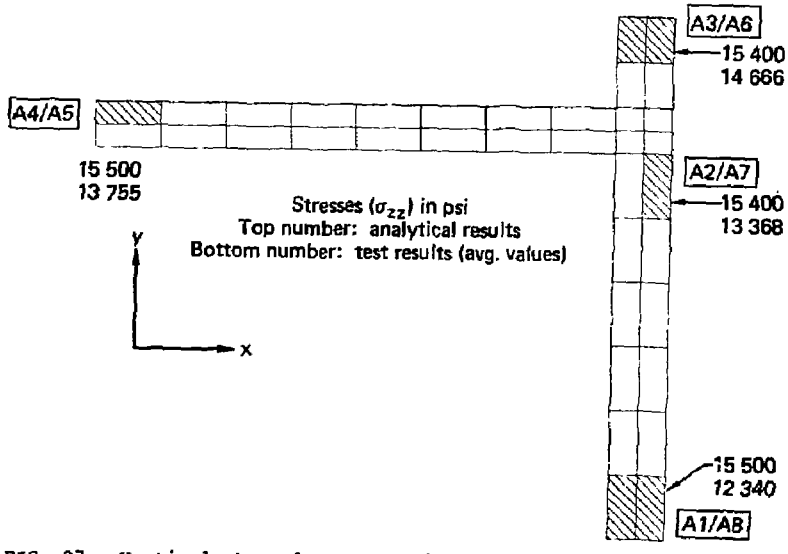

FIG. 27. Vertical channel stresses (σ_{zz}) located 24 in. above the end plate for a channel load of 200 000 lb for the new bolt configuration.

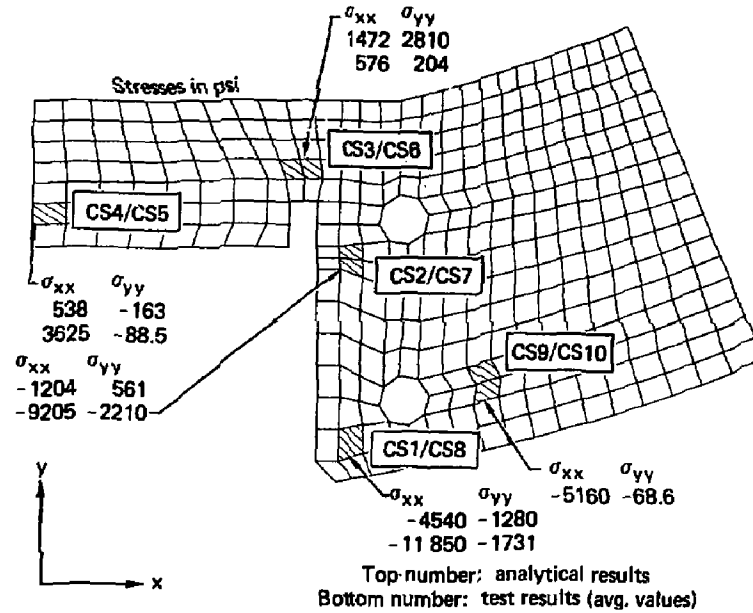

FIG. 28. Horizontal stresses (σ_{xx} and σ_{yy}) for the end plate top surface for a channel load of 200 000 lb for the new bolt configuration.

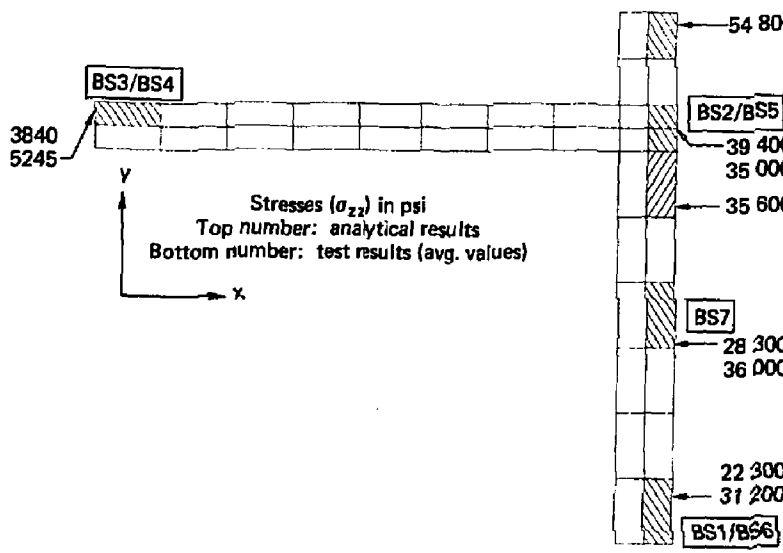

FIG. 29. Vertical stresses (σ_{zz}) for the outside of the channel located 3/4 in. above the end plate for a channel load of 200 000 lb for the new bolt configuration.

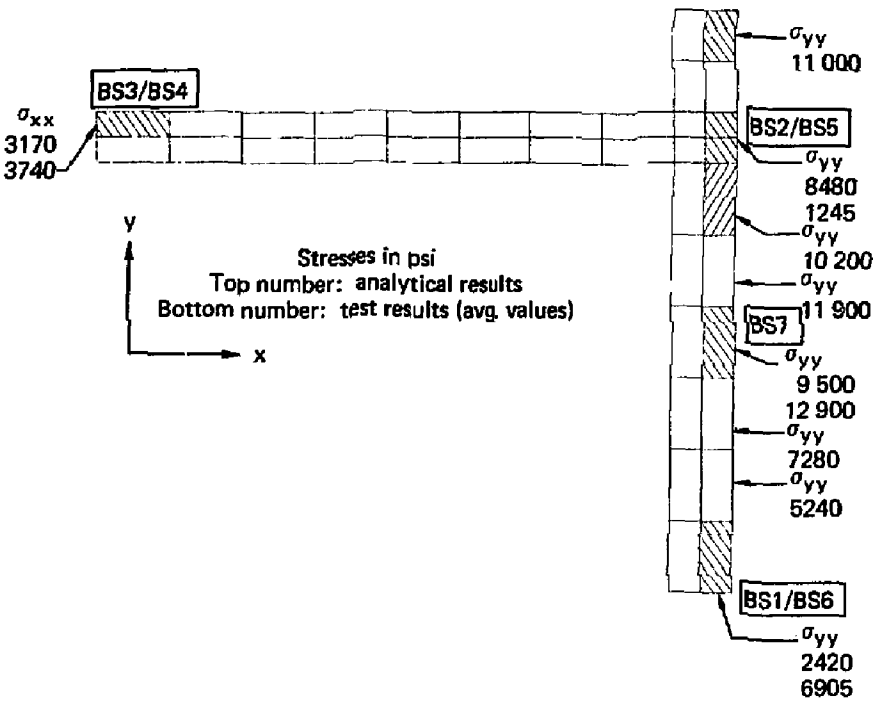

FIG. 30. Horizontal stresses (σ_{xx} and σ_{yy}) for the outside of the channel located 3/4 in. above the end plate for a channel load of 200 000 lb for the new bolt configuration.

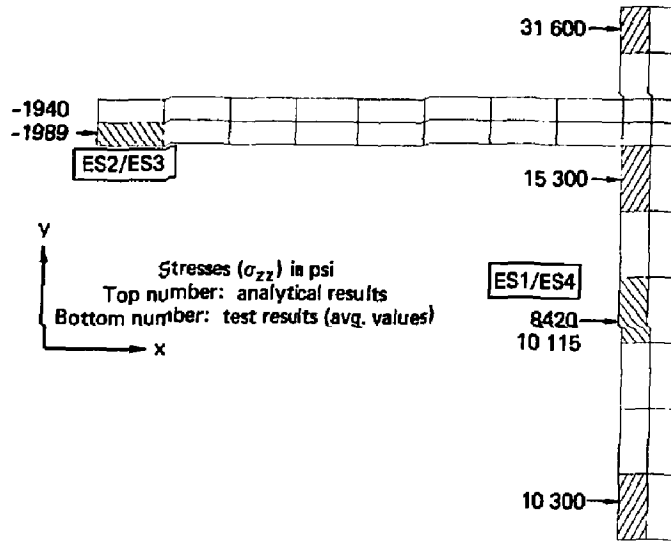

FIG. 31. Vertical stresses (σ_{zz}) for the inside of the channel located 3/4 in. above the end plate for a channel load of 200 000 lb for the new bolt configuration.

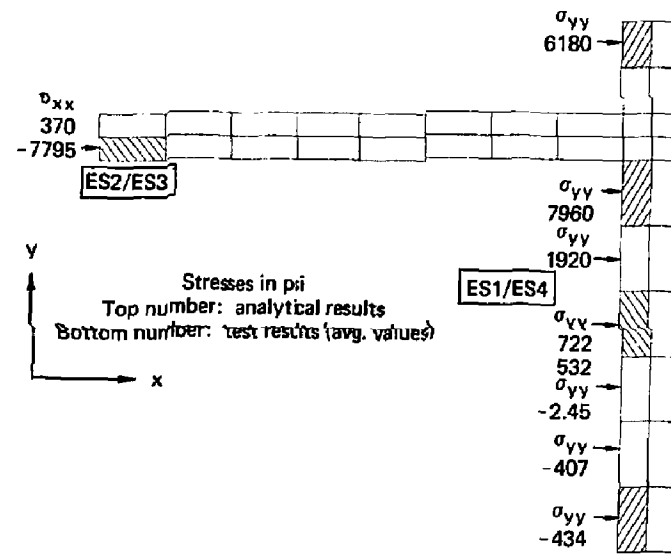

FIG. 32. Horizontal stresses (σ_{xx} and σ_{yy}) for the inside of the channel located 3/4 in. above the end plate for a channel load of 200 000 lb for the new bolt configuration.

stresses (σ_{zz}) compare somewhat better than horizontal stresses (σ_{xx} and σ_{yy}). Overall, the poorest comparisons are for horizontal stresses near the end plate.

COMPARISONS OF TEST RESULTS AND ANALYTICAL SOLUTIONS FOR THE OLD BOLT CONFIGURATION

Comparisons of test and analytical results for the old bolt configuration (100 000-lb channel load) for bolt loads, end plate displacements, and stresses 24 in. above the end plate are given in Ref. 1 and are repeated in Figs. 33 and 34 for ease of reference. Further stress comparisons, at locations identical to those selected for the comparison of data for the new bolt configuration, are given in Figs. 35 through 39. End plate contact area is also given in Ref. 1 and is repeated in Fig. 40.

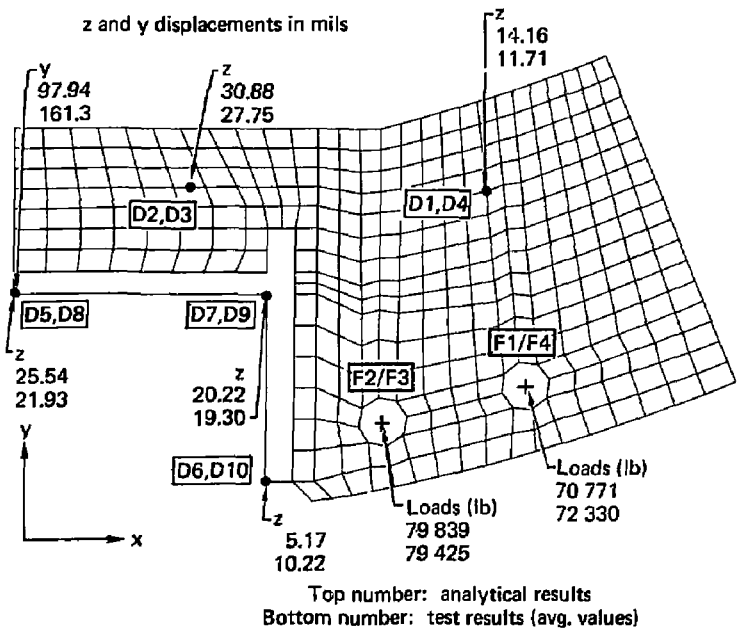

FIG. 33. Bolt loads and end plate displacements for a channel load of 100 000 lb for the old bolt configuration.

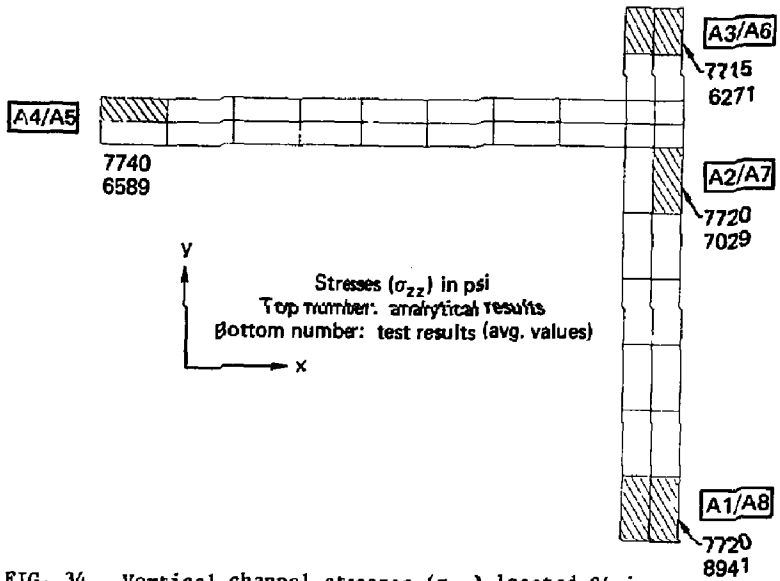

FIG. 34. Vertical channel stresses (σ_{zz}) located 24 in. above the end plate for a channel load of 100 000 lb for the old bolt configuration.

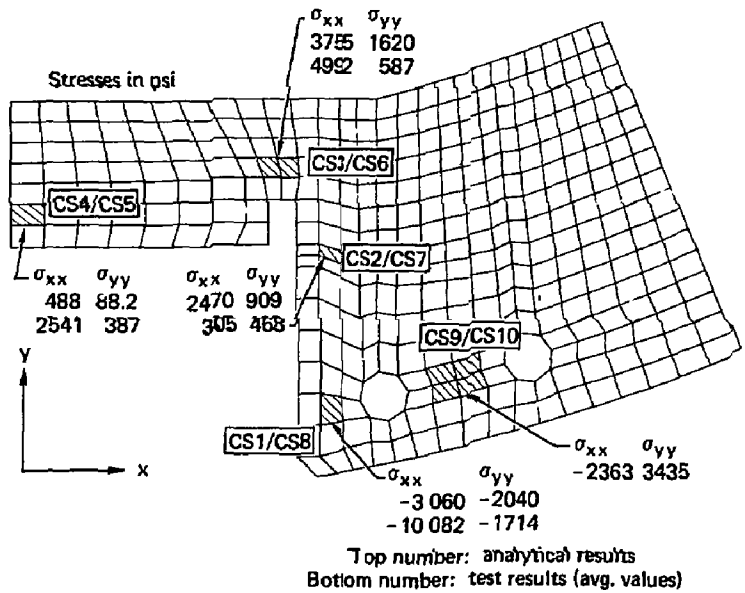

FIG. 35. Horizontal stresses (σ_{xx} and σ_{yy}) for the end plate top surface for a channel load of 100 000 lb for the old bolt configuration.

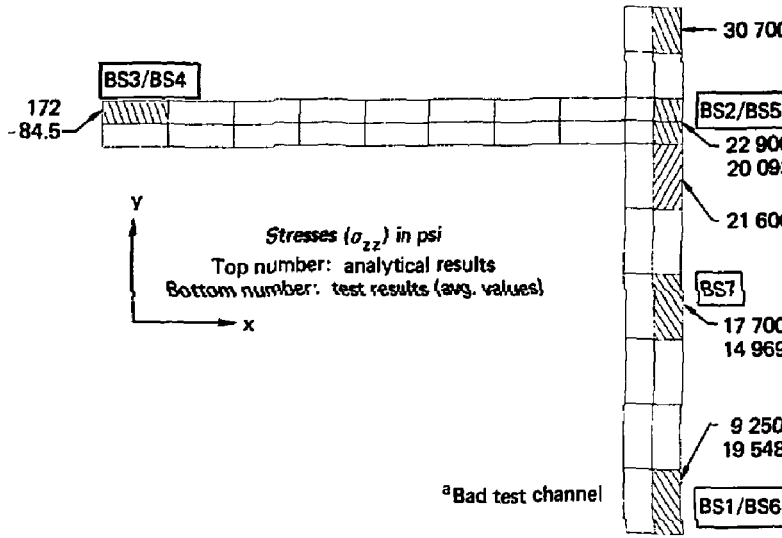

FIG. 36. Vertical stresses (σ_{zz}) for the outside of the channel located 3/4 in. above the end plate for a channel load of 100 000 lb for the old bolt configuration.

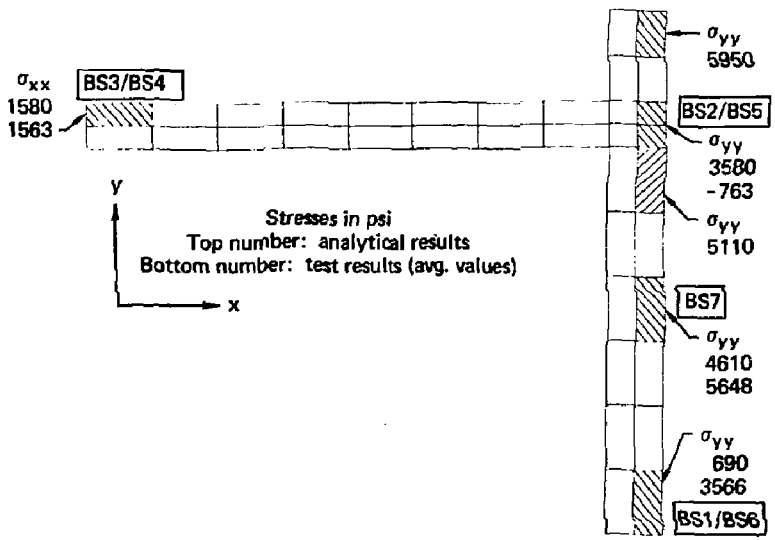

FIG. 37. Horizontal stresses (σ_{xx} and σ_{yy}) for the outside of the channel located 3/4 in. above the end plate for a channel load of 100 000 lb for the old bolt configuration.

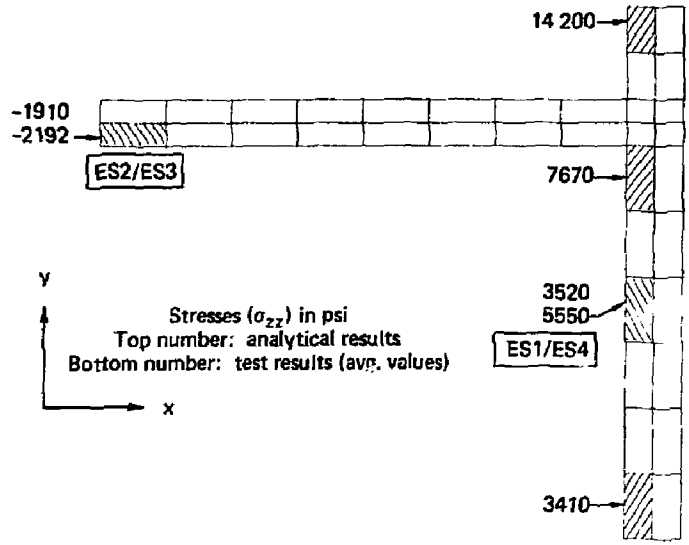

FIG. 38. Vertical stresses (σ_{zz}) for the inside of the channel located 3/4 in. above the end plate for a channel load of 100 000 lb for the old bolt configuration.

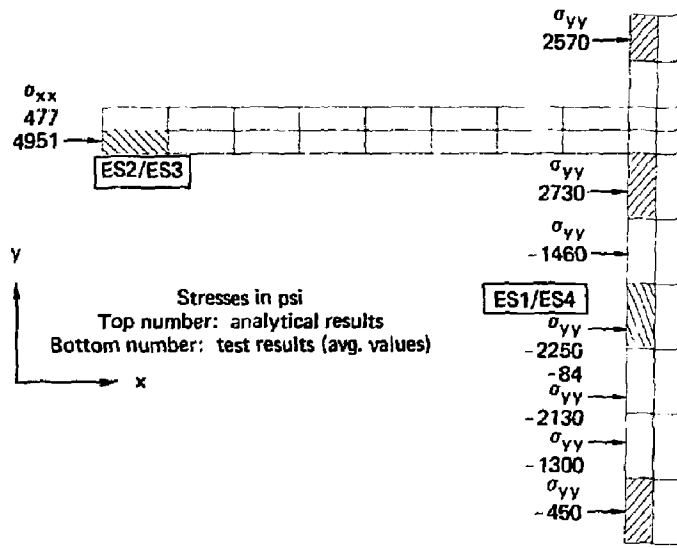

FIG. 39. Horizontal stresses (σ_{xx} and σ_{yy}) for the inside of the channel located 3/4 in. above the end plate for a channel load of 100 000 lb for the old bolt configuration.

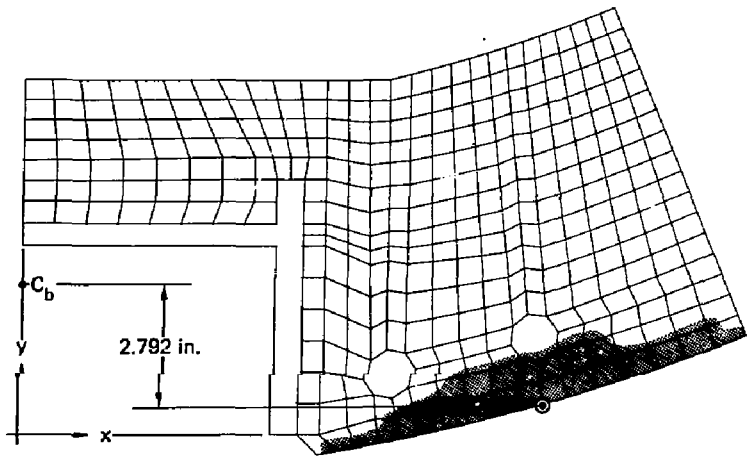

FIG. 40. Final analytical results indicate the shaded interplate contact area for a channel load of 100 000 lb for the old bolt configuration (Ref. 1).

Bolt loads and end plate displacements compare very favorably (Fig. 33) again with the exception of lateral displacement. Stresses at 24 in. above the end plate (Fig. 34) show good correspondence. However, as mentioned before, the channel bending moment, present in test data only, opposes the corresponding moment, for the new bolt configuration, in Test No. 12. Horizontal stresses on the end plate surface show (Fig. 35) poor correlation as do horizontal stresses in the channel near the end plate (Figs. 37 and 39). Vertical stresses in the channel near the end plate show a rough correspondence (Figs. 36 and 38).

Overall, very similar tendencies exist for the correlation of test data and analytical results for both the old and new bolt configurations.

COMPARISONS OF RESULTS FOR OLD AND NEW BOLT CONFIGURATIONS

Direct comparisons for both bolt geometries can be made since results are available for the same channel load, namely 100 000 lb. Figures 19 and 33 indicate that for the new configuration not only are bolt loads reduced but they carry the load more evenly. Also end plate separation is much reduced.

Comparison of Figs. 13 and 40 show that plate contact area is significantly increased. Horizontal stresses on the end plate (Figs. 21 and 35) are significantly reduced and horizontal stresses near the end plate (Figs. 23, 25, 37, and 39) show the same general tendencies as in Figs. 12 and 18 except that analytical results indicate bending occurs along a shorter length of the flange for the new bolt configuration. Also, as mentioned before, test results show the horizontal channel bending moment significantly reduced (Figs. 20 and 34).

Comparison of bolt geometries for the statics of the connection (Fig. 11) indicates that for the new bolt configuration the interplate bearing force $\vec{A}$ is reduced (due to reduced bolt loads) from 212 800 to 198 600 lb for test results and from 200 200 to 179 100 lb for analytical results. The moment, due to the location of the bolts $\vec{M}_e$ and its equilibrating moment, due to the location of the interplate bearing force, is likewise reduced from 46 850 to 4270 ft-lb and from 46 600 to 3780 ft-lb for test and analytical results, respectively. Finally, the interplate bearing force, for the new bolt geometry is located much closer to the channel centroid away from the edge of the end plate, from y_a = 2.412 in. to y_a = 0.2576 in. for test results and from y_a = 2.792 in. to y_a = 0.2532 in. for analytical results. This is consistent with the y coordinates for the centroid of the contact surface as observed in Figs. 13 and 40.

SUMMARY AND CONCLUSIONS

Test and analysis of the described newly configured bolted connection (Fig. 3) for both 100 000- and 200 000-lb channel loads have been presented. Results from an analogous study (100 000-lb channel load only) for the connection as originally designed (Fig. 2) are referenced. Correspondence of results for test and analysis is reasonably good for bolt loads, end plate displacements, and stresses located a distance from the welded channel end plate connection. Poorer correlation exists for results close to the weld. These remarks hold true for both bolt configurations.

The new bolt pattern for the connection has several advantages over the old design, including reduced and more evenly distributed bolt loads, smaller end plate separation and significant reduction of end plate horizontal stresses. Also, the interplate bearing force and moment are significantly

reduced. The plate contact area is increased substantially and its centroid location provides for increased static stability of the connection.

Analysis of the true canister configuration, as recommended in Ref. 1, including the required additional end plate constraints, would be of definite value.

REFERENCES

1. Michael A. Gerhard, Diagnostic Test Systems Canister Weld Joint Analysis, Lawrence Livermore National Laboratory, Livermore, CA, UCID-18750 (1981).
2. S. J. Sackett, Users Manual for SAP4 A Modified and Extended Version of the U.C. Berkeley SAPIV Code, Lawrence Livermore National Laboratory, Livermore, CA, UCID-18226 (1979).
3. Michael A. Gerhard, SLIC: An Interactive, Graphic Mesh Generator, for Finite-Element and Finite-Difference Application Programs, Lawrence Livermore National Laboratory, Livermore, CA, UCRL-52823 (1979).

RD/kt

APPENDIX A.

In order to fully document the analytical results, Table A-1 gives the input, output, and SLIC model files and their directory locations for the various solutions presented in the text. Also, as an aid in verification of results, the detailed geometry of the channel/end plate joint is given in Fig. A-1. Complete scaled drawings are available from EG&G, P. O. Box 204, San Ramon, CA 94583.

TABLE 1-A. Input, output, and SLIC model files and their directory locations for analytical solutions considered in the text.

Solution	SLIC model	Input	Output	Directory
New bolt configuration (100 K[a] channel load)	SLIC-14	SAP4I-18D	SAP40-18D	.310938:LLIFE:M:TSTP10
New bolt configuration (200 K channel load)	SLIC-14	SAP4I-19B	SAP40-19B	.310938:LLIFE:M:TSTP11
Bolt preload new configuration	SLIC14P	SAP4IP-7	SAP40P-7	.310938:LLIFE:M:TSTP6
Old bolt configuration (10 K channel load)	SLIC-13	SAP4I-13D	SAP40-13D	.310938:LLIFE:M:TSTP4
Bolt preload old configuration	SLIC12B	SAP4I-12A	SAP40-12A	.310938:LLIFE:M:TSTP

[a] 1 K = 1000 lb.

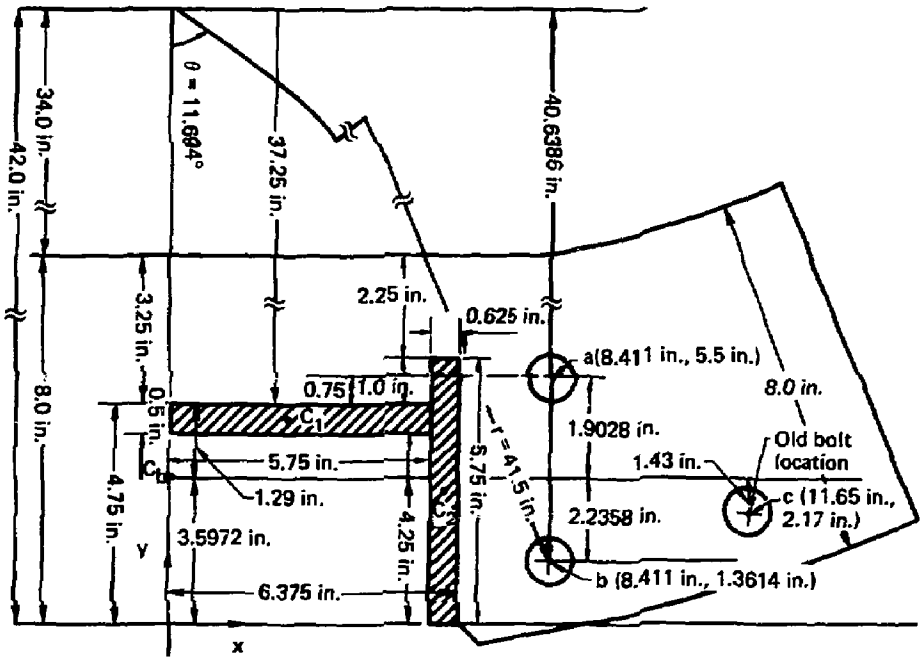

FIG. A-1. Channel/end plate geometry. The channel centroid locations, C_b is the point through which both the test specimen and the analytical model are loaded. Points a and b define the new bolt configuration and points b and c define the old bolt configuration.